Electromagnetic Eddy Current Sensors for Evaluation of Sea-Cure and 2205 Duplex Condenser Tubing

K. KRZYWOSZ, H. HENAFF and M. MAYOS

ABSTRACT

As more condenser tubes are replaced with high performance, thin-walled ferritic stainless steel tubing such as Sea-Cure and 2205 duplex, more attention is needed to address inspectability of such tubing, especially in both tube free spans and tubes under support plates. EPRI has been examining this issue by evaluating both mockups and field-removed tubes, and by conducting field trials utilizing both magnetically-saturating eddy current probes as well as combination Saturn probes that inspect and characterize both tube free spans and tubes under support plates using innovative probe designs.

This paper presents results of one such evaluation by reviewing a field-removed Sea-Cure tube section containing impingement pits in a steam eroded condenser tube section. Also, details of the 2205 duplex tubing mockup evaluation will be presented based on the application of both magnetically-saturating eddy current and combination Saturn probes.

INTRODUCTION

The first part of the presentation involves evaluation of a field-removed condenser section made of Sea-Cure tubing affected by steam erosion and impingement pits: 0.750” outer diameter (OD) by 0.028” nominal wall. This is followed by the mockup evaluation of 2205 duplex tubing with 0.787” OD by 0.020” nominal wall containing known planer and volumetric flaws at both tube free spans and at tube-to-tube support plate intersections. It should be noted that both tube types are ferromagnetic with relative permeability values in the range of 30-100 [1]. Two different material types were utilized for support plates: Type 304 stainless steel for Sea-Cure tubing and Type 283, Grade C, carbon steel for 2205 duplex tubing. Additional details regarding the use of 2205 duplex tubing for condensers at Electricité de France (EDF) nuclear plants are presented elsewhere [2].

Kenji Krzywosz, Electric Power Research Institute (EPRI), 1300 W.T. Harris Blvd., Charlotte, NC 28262 USA
Herve Henaff, Electricité de France (EDF), Dept. ETUDES - Service ECE 2 rue Ampère 93206 Saint-Denis Cedex 01 France
Michel Mayos, Electricité de France (EDF), Nuclear Operation Engineering Support, 1 Place Pleyel 93282 Saint-Denis Cedex France

To compensate for the ferromagnetic tube wall, a series of permanent magnets were placed next to differential bobbin coils to axially saturate the tube wall.This basically allowed establishment of phase angle-to-flaw depth calibration curves at selected operating frequencies. The combination probe, in addition to the magnetically-saturating bobbin coils, housed a set of six pancake array coils between the two transmitting bobbin coils to allow tube inspections under tube support plates. This was accomplished in a partial-saturation, transmit-receive mode.

SEA-CURE REFERENCE STANDARD

Prior to evaluating the field-removed Sea-Cure condenser tube section, a reference standard was fabricated to establish both the instrument gain and phase angle settings to establish appropriate calibration curves. The resultant standard shown below as Figure 1 contained both OD pits and wall thinning.

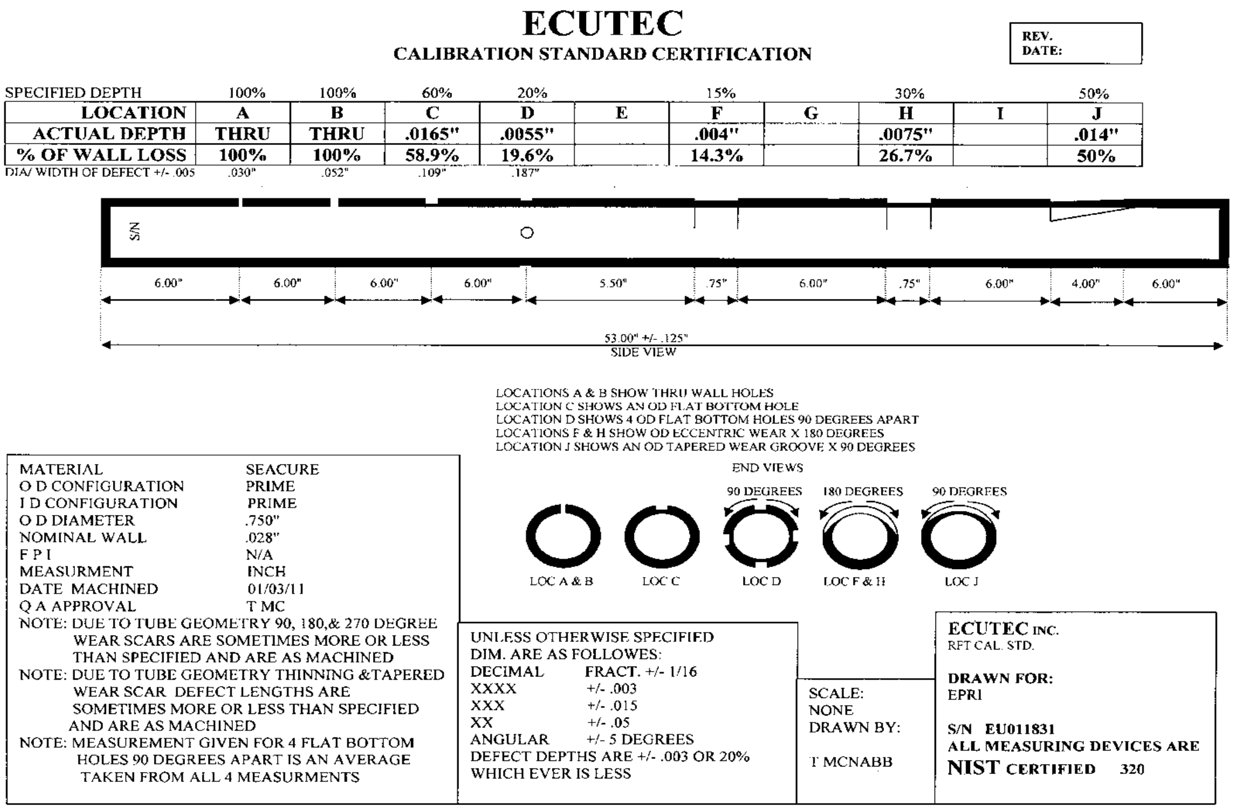

Figure 1. Sea-Cure Calibration Standard Drawing.

SEA-CURE CALIBRATION STANDARD EDDY CURRENT SIGNALS

To assess and evaluate the impingement pit detection and sizing capabilities, a magnetically-saturating bobbin probe was selected for this evaluation. This allowed phase angle-based analysis to be performed by correlating obtained phase angles to respective flaw depth information. The overall phase angle spread for 100% to 20% holes was around 65° at 500 kHz. At 100 kHz, the phase angle spread was reduced to 22°.

Two respective calibration curves were established: one for estimating OD pits at 500 kHz using phase angles and another for estimating OD wall thinning at 50 kHz using $Vert_{max}$ amplitude. For these curves, a dent placed in the removed tube section was used by setting the dent signal to horizontal and allowing the 100% signals to rotate accordingly.

EDDY CURRENT EVALUATION OF FIELD-REMOVED SEA-CURE CONDENSER TUBE SECTION

The utility-furnished field-removed tube section was approximately 46.5" long. Figure 2 shows an expanded view of the entire tube section showing one of the larger pits within steam eroded tube area complete with a tube support plate ring simulating the tube support plate.

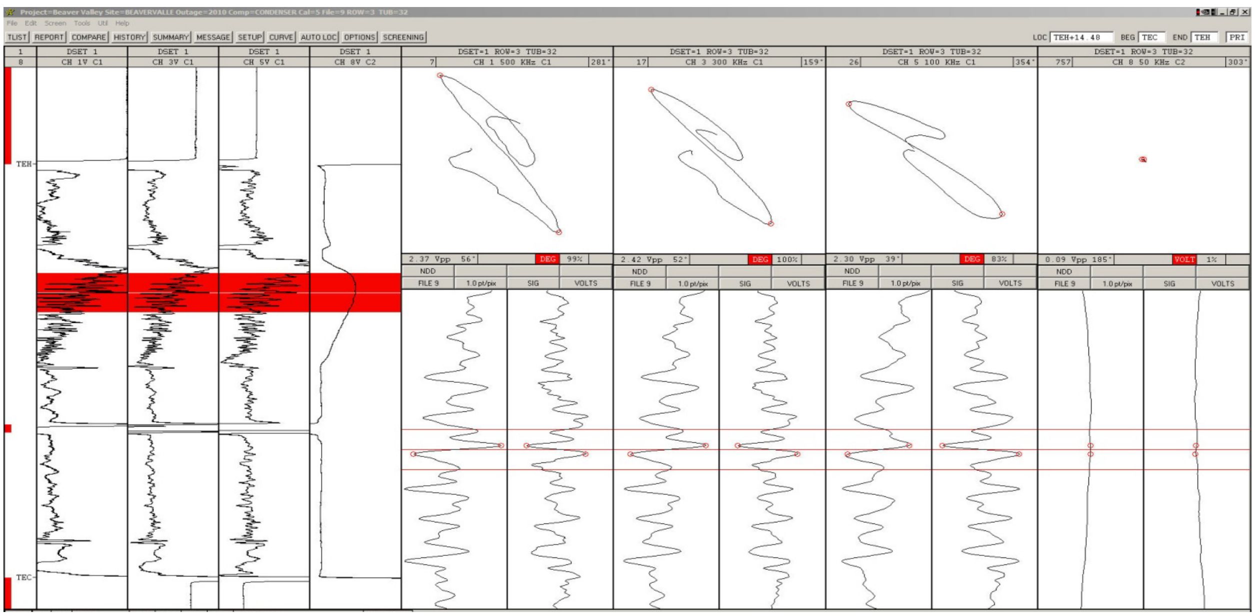

Figure 2. Pit #4 at TEH+15.03" – 99% Wall Loss Estimate.

Based on the setup, the resultant Type 304 stainless steel support signal at 500 kHz was approximately five times greater in amplitude compared to a through-wall signal. However, unlike the carbon steel support plate signal, it was possible to perform a support plate mix which brought the mix residual signals to under 0.5 volt.

Basically, the steam impingement pit signals of interest were confined to within the steam erosion area as shown by the absolute drift signal of 50 kHz, Channel 8. The tube area of interest was cut at the beginning of tube erosion where it was marked with a tube ding.

DESTRUCTIVE SECTIONING RESULTS

To compare and ascertain the depth of impingement pits, six pits were selected from the steam erosion area for destructive sectioning analyses. Table 1 shows the percent wall losses by destructive sectioning results of six identified pits along with the eddy current estimates. Along with the furnished pit depths, nearby pit wall thickness values were also provided. The averaged pit depths in the steam-eroded area were 81% while the nearby steam erosion wall loss was averaged to be 31%.

Table 1. Pit/Wall Loss Results.

Pit Number	Nearby % Wall Loss	Pit Depth Estimate (% Loss)	Eddy Current Estimate (% Loss)
#1	35	60	73
#2	34	88	99
#3	39	78	97
#4	41	86	99
#5	18	79	99
#6	17	93	99
Average	31%	81%	94%

2205 DUPLEX REFERENCE STANDARD

For the mockup evaluation with the combination Saturn probe, a similar standard made of 2205 duplex tubing was fabricated. It was the same as the Sea-Cure standard except for the additional 20% OD and 20% ID grooves present in the reference standard.

The magnetically-biased bobbin probe was operated in both differential and absolute impedance mode at operating frequencies of 650, 400, 200, and 100 kHz, while six pancake coils were operated in a partial-saturation, transmit-receive, mode. Only the differential coil data was acquired by six individual pancake coils at frequencies of 50, 30, 15, and 10 kHz.

For evaluating free-span tube regions, the magnetically-biased bobbin coil data from 650 kHz was used to establish the flaw depth sizing curve based on the measured phase angles. Since the pancake coils were operated in a partial-saturation mode, no phase angle-based flaw depth sizing was possible at tube-to-tube support plate intersections. Instead, the individual pancake coil data, especially at 50 kHz, was used to confirm the presence of tubing flaws under support plates.

Individual phase angles were set up based on placing the background tube noise signal to horizontal and allowing the individual flaw signals to orient accordingly to establish the differential phase angle curves. Based on the optimum phase spread, the 650 kHz phase angle curve was used to estimate the free-span tubing flaws.

Similarly, individual pancake coils were set up by placing the background tube noise to be horizontal on each of six pancake coil channels at four operating frequencies. It should be noted that nominal support plate signals based on individual pancake coil channels differed in shape and amplitude due to the combined effect of background tube noise and orientation of the individual coils relative to each support plate.

MOCKUP EVALUATION BY COMBINATION SATURN PROBE

Based on the above setups, the 9-tube mockup was tested and evaluated with the combination probe. All free-span tubing flaws ranging in flaw depths of 24% to 100% were detected and sized with the magnetically-biased bobbin probe section of the Saturn probe. The depth sizing for the population of 24 different flaw types fell short of desirable sizing results with the overall correlation coefficient of 78% with standard error estimate of 18% as shown in Figure 3. For ferromagnetic materials, our desired goal is to have 80% or higher correlation coefficient with 15% or lower standard error of estimate. The figure shows that deeper flaws were better sized than shallower flaws of 50% and below.

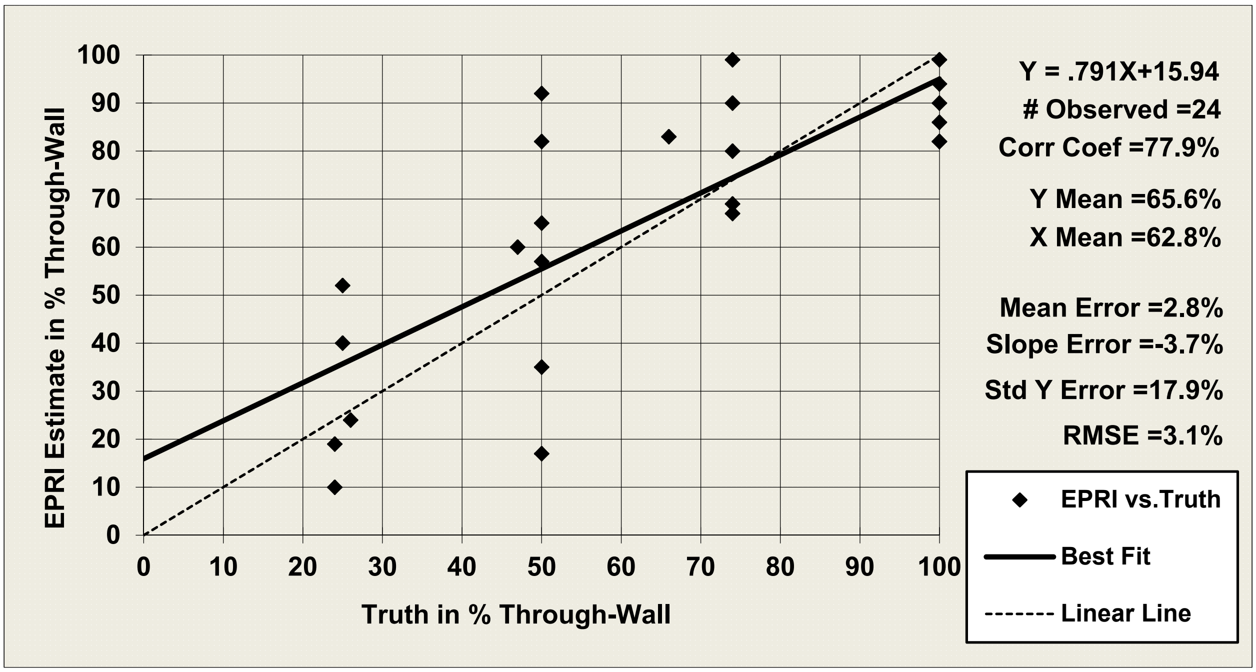

Figure 3. Regression Plot Showing Free-Span Flaw Sizing Performance of Combination Saturn Probe.

Review of individual pancake coils showed that it was possible to identify the majority of deeper flaws under support plates, such as wear and axial/circumferential flaws. However, it was not possible to identify smaller diameter pit-like flaws, including a through-wall pit under a support plate. The overall flaw detection capabilities under support plates are tabulated as Table 2 showing which flaw types and flaw sizes were detected by six pancake array coils operated at 50 kHz. Of 18 flaws having greater than 20% wall losses under tube supports, the overall flaw detection percentage was 61%. This detection sensitivity increased to 75% by considering only 50% and higher wall losses.

Table 2. Summary of Under Support Flaw Detections by Saturn Probe.

Flaws Under Support Plate	Saturn Probe-Based Signal Detection (50 kHz)
1-2: 21% Uniform Wear Under #2 TSP	No
1-2: 39% Uniform Wear Under #3 TSP	Yes
1-2: 61% Uniform Wear Under #4 TSP	Yes

2-1: 24% Axial Notch Under #1 TSP	No
2-1: 50% Axial Notch Under #2 TSP	Yes
2-1: 76% Axial Notch Under #3 TSP	Yes
2-1: 100% Axial Notch Under #4 TSP	Yes
2-2: 24% Circ Notch Under #1 TSP	No
2-2: 50% Circ Notch Under #2 TSP	No
2-2: 82% Circ Notch Under #3 TSP	Yes
2-2: 100% Circ Notch Under #4 TSP	Yes
2-3: 26% Tapered Wear Under #1 TSP	Yes
2-3: 50% Tapered Wear Under #2 TSP	Yes
2-3: 66% Tapered Wear Under #3 TSP	Yes
3-2: 100% Pit Under #1 TSP	No
3-2: 100% Tube Cut Under #2 TSP	Yes
3-2: 50% ID Pit Under #3 TSP	No
3-2: 25% ID Pit Under #4 TSP	No

VENDOR PERFORMANCE OF 2205 TUBING MOCKUP

The vendor relied primarily on 1MHz differential channel for flaw depth sizing. Other frequencies included 500 kHz absolute, 200 kHz differential, and 100 kHz differential based on using a TC 5700 eddy current tester. The flaw depth sizing curve was established using a magnetically-saturating bobbin probe that was manufactured by Exceldef. Based on the selected operating frequency of 1 MHz, a 90-degree phase angle separation was attained between the 10% ID and 10% OD grooves. The overall system was set up on four by 1mm in diameter through-wall holes at respective amplitude/phase angle settings of 1 volt at -25°.

All free-span tubing indications were detected using the magnetically-biased bobbin probe. To assess the sizing performance, the same 2205 duplex tubing mockup was tested at the vendor facility site using their TC 7700 eddy current tester. Using a mechanical pusher/puller, the mockup tubing data was obtained at an inspection speed of 20” per second.

Figure 4 shows the overall sizing performance in a regression plot. The overall sizing performance showed slight improvements over the Saturn probe. Namely, the correlation coefficient increased to 84% (from 78%) with a reduced standard estimate of sizing error to 17% (from 18%).

One negative aspect of the sizing performance was the tendency of the system to undersize or be less conservative in making analysis calls. As the figure indicates, analysis calls were systematically under-estimated by approximately 17%. In practice, it’s better to be more on the conservative side to allow tubes to be plugged or repaired to preclude any unscheduled shut-downs due to possible tube leaks.

Table 3 shows a similar flaw detection performance as in Table 2 at tube-to-tube support plate intersections. As expected, due to larger and variable tube support plate signals caused by stronger magnetic field to carbon steel interactions, the overall flaw detection sensitivity at tube support plate locations was reduced to 28%. By considering tubing flaws equal to or greater than 50% wall losses under supports, the detection sensitivity increased slightly to 33%.

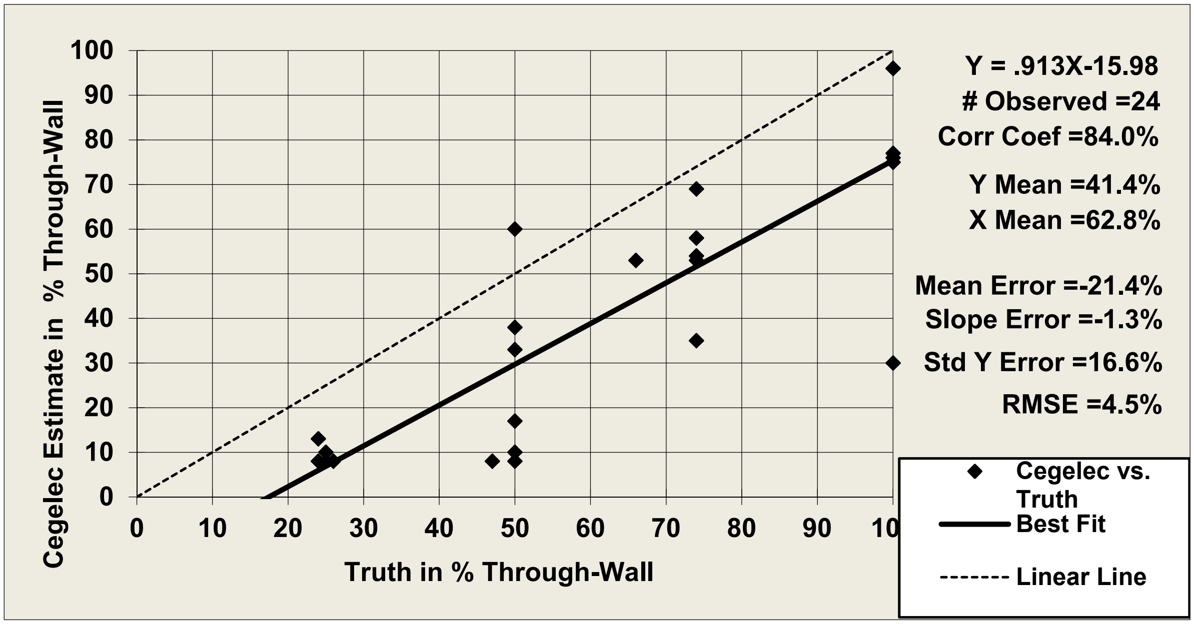

Figure 4. Regression Plot Showing Free-Span Flaw Sizing Performance of Exceldef Probe.

Table 3. Summary of Under Support Flaw Detections by Exceldef Probe.

Flaws Under Support Plate	Exceldef Probe-Based Signal Detection (100 kHz)
1-2: 21% Uniform Wear Under #2 TSP	No
1-2: 39% Uniform Wear Under #3 TSP	Yes
1-2: 61% Uniform Wear Under #4 TSP	Yes
2-1: 24% Axial Notch Under #1 TSP	No
2-1: 50% Axial Notch Under #2 TSP	No
2-1: 76% Axial Notch Under #3 TSP	No
2-1: 100% Axial Notch Under #4 TSP	Yes
2-2: 24% Circ Notch Under #1 TSP	No
2-2: 50% Circ Notch Under #2 TSP	No
2-2: 82% Circ Notch Under #3 TSP	No
2-2: 100% Circ Notch Under #4 TSP	No
2-3: 26% Tapered Wear Under #1 TSP	No
2-3: 50% Tapered Wear Under #2 TSP	Yes
2-3: 66% Tapered Wear Under #3 TSP	Yes
3-2: 100% Pit Under #1 TSP	No
3-2: 100% Tube Cut Under #2 TSP	No
3-2: 50% ID Pit Under #3 TSP	No
3-2: 25% ID Pit Under #4 TSP	No

SUMMARY

The following observations are presented based on the inspection results of both Sea-Cure and 2205 ferritic tubing.

- Based on the six impingement pits found in the presence of steam erosion in Sea-Cure tubing, the averaged eddy current pit depth estimates were 94% in comparison to 81% by destructive sectioning results.
- The estimated maximum steam erosion by eddy current was 42% versus averaged wall thinning of 31% with maximum wall thinning of 41%.
- Magnetically-saturating eddy current probe was used successfully to characterize both impingement pits and steam erosion in free-span tube regions.
- For 2205 duplex tubing, use of a magnetically-biased probe by the vendor showed better overall sizing performance of free-span tubing flaws with correlation coefficient of 84% with standard error estimate of 17%.
- Detection performance under support plates showed an overall detection percentage of 61% and 75% for flaws equal to or greater than 20% and 50% wall losses, respectively, for pancake coils; the similar but lower detection percentages of 28% and 33% were noted by the magnetically-biased bobbin coils.
- Enhanced flaw detection and sizing capabilities by the combination Saturn probe were demonstrated using the 2205 duplex tubing mockup.

REFERENCE

1. K. Krzywosz, Nondestructive Evaluation: Advanced Nondestructive Evaluation Methods for Testing Ferritic and Duplex Tubing, EPRI Report 1022932, October 2011.
2. M. Mayos, NDE Issues in the Inspection of Duplex Stainless Steel Condenser Tubes, Presented at 11th EPRI Balance-of-Plant Heat Exchanger NDE Symposium, Stevenson, WA, August 9-11, 2010.